Numerical Investigation on Applicability of j_C-Measurement Method to Multiple High-Temperature Superconducting Tape*)

Takazumi YAMAGUCHI[1)], Hiroaki OHTANI[1,2)], Shinsuke SATAKE[1,2)], Nagato YANAGI[1,2)] and Yuta ONODERA[2)]

[1)]*The Graduate University for Advanced Studies, Toki 509-5292, Japan*
[2)]*National Institute for Fusion Science, Toki 509-5292, Japan*

(Received 9 January 2022 / Accepted 18 February 2022)

A numerical code has been developed in order to investigate the applicability of the permanent magnet method to vertically-stacked multiple high-temperature superconducting (HTS) tapes. The permanent magnet method was proposed to simply and contactlessly measure the critical current density in the HTS tape. By this method, the critical current density is estimated from the proportional relation between the critical current density and the Lorentz force working on the permanent magnet. The Maxwell equation, coupled with the superconductivity characteristics, is solved by the edge-based finite element method to investigate the effect of the number of HTS tapes on the Lorentz force. As a result, it is clear that the permanent magnet method can be applied to measurement of the critical current density in the multiple HTS tapes although there is an upper limit of the number of HTS tapes in which the critical current density can be measured. In addition, by using stronger magnet, the permanent magnet method can measure the critical current density when more number of HTS tapes are stacked.

Keywords: contactless method, critical current density, edge-based finite element method, numerical simulation, high-temperature superconducting film

DOI: 10.1585/pfr.17.2405035

1. Introduction

Recently, the application of a high-temperature superconducting (HTS) tape to an electromagnet for fusion reactors has attracted attention [1, 2]. In an HTS tape, an HTS layer is piled with a stabilizing layer made of Cu and/or Ag on a material substrate made of Hastelloy (see Fig. 1). If defects such as clacks and/or small holes exist in the HTS tape, the superconductivity performance deteriorates locally. As one of the physical parameters characterizing the superconductivity, the critical current is widely known. The critical current is a maximum electric current which can flow in a superconductor. It is necessary to develop a method to measure the critical current in the HTS tape.

As a simple and contactless measurement method, Ohshima *et al.* proposed the permanent magnet method [3, 4]. A permanent magnet is arranged above an HTS sample, cooled by liquid nitrogen, and moves down and up (see Figs. 2 (a) and 2 (b)). When the permanent magnet approaches the HTS sample, a shielding current is induced in the HTS sample to shield the applied magnetic field generated by the permanent magnet (see Fig. 2 (a)). Then, a repulsive force acts on the permanent magnet. When the permanent magnet leaves the HTS sample, the reverse shielding current is induced to conserve a magnetic field in the HTS sample (see Fig. 2 (b)). Then, an attractive force acts on the permanent magnet. If the HTS sample is exposed to a sufficiently large magnetic field, so that the shielding current becomes equal to the critical current, then the repulsive force is proportional to the critical current. Hence, the critical current can be estimated from the repulsive force. Ohshima *et al.* experimentally confirmed the proportional relation between the critical current and the repulsive force [3, 4]. Takayama *et al.* numerically confirmed the proportional relation [5]. The HTS sample used in these studies was a single layer HTS film. On the other hand, an HTS conductor used in the HTS magnets is made vertically-stacked multiple HTS tapes. However, it is not clear whether the permanent magnet method can estimate the critical current in the multiple HTS tapes.

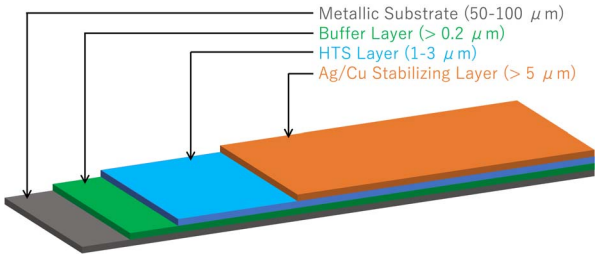

Fig. 1 A schematic view of the HTS tape.

The purpose of the present study is to develop a

author's e-mail: yamaguchi.takazumi@nifs.ac.jp

*) This article is based on the presentation at the 30th International Toki Conference on Plasma and Fusion Research (ITC30).

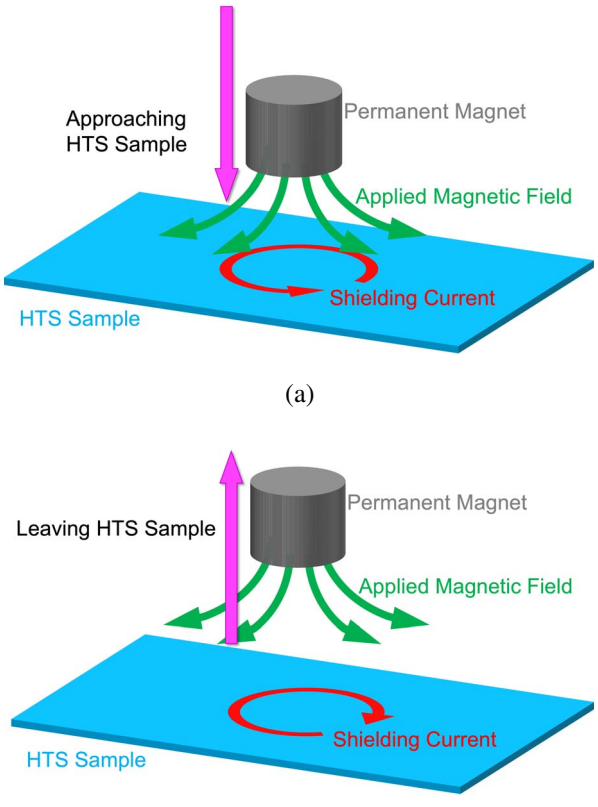

Fig. 2 A schematic view of the permanent magnet method.

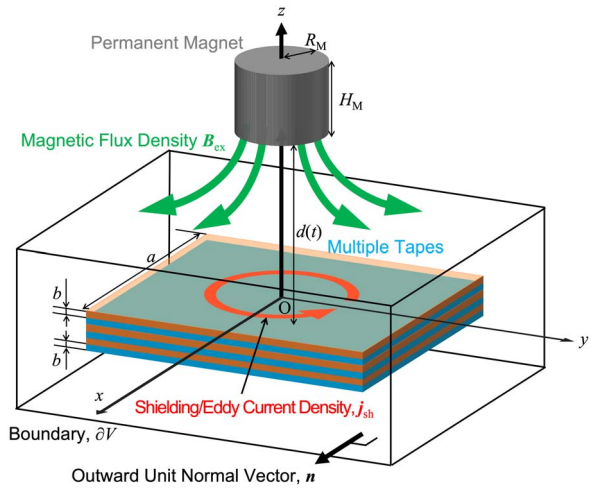

Fig. 3 The FEM model of the permanent magnet method for the case with $L = 3$. In this figure, the orange and light blue tapes show the stabilizing and HTS layers of the HTS tape, respectively. There is only the applied magnetic flux density $\boldsymbol{B}_{ex}$ on the boundary ∂V.

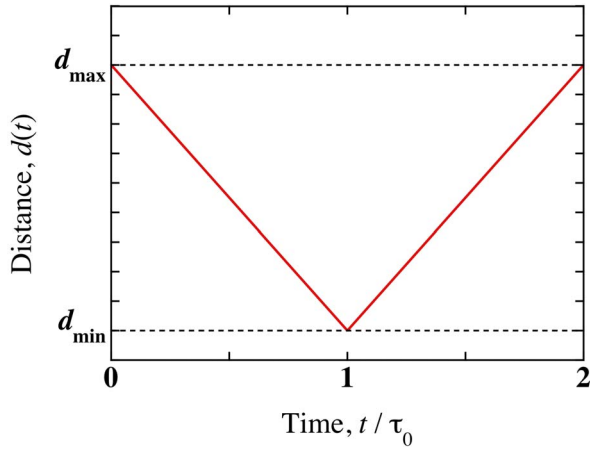

Fig. 4 Time dependence of the distance $d(t)$ between the magnet bottom and the tape surface.

numerical code based on the edge-based finite element method (FEM) for analyzing the electromagnetic field and the shielding current in multiple HTS tapes. Moreover, the applicability of the permanent magnet method to the multiple HTS tapes is investigated by using the numerical code.

2. Governing Equation and Numerical Method

The FEM model of the permanent magnet method is shown in Fig. 3. Throughout the present study, we assume that the electromagnetic effect of the metallic substrate and the buffer layer is neglected. This is because the HTS layer and the metal substrate are insulated by the buffer layer. Moreover, the shape of the HTS tape is a square of thickness $2b$ and length a on one side. In other words, the thicknesses of both the stabilizing and HTS layers are b. The upper and lower surfaces of the multiple HTS tapes are located at $z = 0$ and at $z = -2Lb$, respectively, where L is the number of the HTS tapes. Moreover, the HTS tapes are exposed to a magnetic flux density $\boldsymbol{B}_{ex}$ generated by a permanent magnet. The shape of the permanent magnet is a cylinder of radius R_M and height H_M. The center of the magnet bottom is located at $(x, y, z) = (0, 0, d(t))$. The distance $d(t)$ between the magnet bottom and the tape surface is controlled, as shown in Fig. 4. After the permanent magnet approaches the HTS tape at a constant speed of τ_0 sec, it leaves the HTS tape at the same speed. Moreover, for an index to show the strength of the permanent magnet, we use a magnetic flux density B_0 at $(x, y, z) = (0, 0, 0)$ for the case with $d = d_{min}$.

Under the above condition, the shielding current density $\boldsymbol{j}_{sh}$ is calculated by solving the following Maxwell equation [6, 7]:

$$\begin{cases} \nabla \times \boldsymbol{E} = -\dfrac{\partial \boldsymbol{B}}{\partial t} \\ \nabla \times \left(\dfrac{1}{\mu_0} \boldsymbol{B} \right) = \boldsymbol{j} \\ \nabla \cdot \boldsymbol{B} = 0 \\ \boldsymbol{j} = \boldsymbol{j}_{sh} + \boldsymbol{j}_{ex} \end{cases} . \tag{1}$$

Here, $\boldsymbol{E}$ and $\boldsymbol{B}$ are the electric field and magnetic flux density, respectively. Moreover, μ_0 is magnetic permeability in a vacuum. Furthermore, $\boldsymbol{j}_{ex}$ is the source current density

generating the applied magnetic flux density $\boldsymbol{B}_{\rm ex}$ and satisfies Ampère's law: $\boldsymbol{j}_{\rm ex} = \nabla \times (\boldsymbol{B}_{\rm ex}/\mu_0)$. Note that $\boldsymbol{j}_{\rm sh}$ is a function of position. Namely, $\boldsymbol{j}_{\rm sh}$ in the HTS layer denotes the shielding current density, and $\boldsymbol{j}_{\rm sh}$ in the stabilizing layer denotes the eddy current density. In addition, as initial and boundary conditions of the Maxwell equation, we assume the following conditions:

$$\boldsymbol{j}_{\rm sh} = \boldsymbol{0} \quad \text{at} \quad t = 0, \tag{2}$$

$$\boldsymbol{B} \cdot \boldsymbol{n} = \boldsymbol{B}_{\rm ex} \cdot \boldsymbol{n} \quad \text{on} \quad \partial V. \tag{3}$$

Here, $\boldsymbol{n}$ is the outward unit normal vector on the boundary ∂V (see Fig. 3). The initial condition (2) shows that the shielding current does not exist in the HTS tapes at $t = 0$. The boundary condition (3) shows that a magnetic flux density of the shielding current does not exist on the boundary ∂V.

The shielding current density $\boldsymbol{j}_{\rm sh}$ in the HTS layer nonlinearly depends on the electric field $\boldsymbol{E}$. Throughout the present study, as the J–E constitutive relation representing the superconductive characteristics, we adopt the following critical-state model [6]:

$$\begin{cases} \boldsymbol{j}_{\rm sh} = \dfrac{j_{\rm C}}{|\boldsymbol{E}|}\boldsymbol{E} & (|\boldsymbol{E}| \neq 0) \\ \dfrac{\partial \boldsymbol{j}_{\rm sh}}{\partial t} = \boldsymbol{0} & (|\boldsymbol{E}| = 0) \end{cases}. \tag{4}$$

Here, $j_{\rm C}$ is the critical current density. On the other hand, in the stabilized layer consisting of Cu/Ag, Ohm's law is satisfied:

$$\boldsymbol{j}_{\rm sh} = \sigma \boldsymbol{E}, \tag{5}$$

where σ is the electric conductivity in the stabilizing layer. Throughout the present study, σ in the stabilizing layer is fixed as $\sigma = 10^8$ S/m.

Before discretizing the Maxwell equation (1) with the edge-based FEM, the Maxwell equation (1) is transformed by using the A-formulation [7, 8]. The total magnetic flux density $\boldsymbol{B}$ is divided into two terms: $\boldsymbol{B} = \boldsymbol{B}_{\rm ex} + \boldsymbol{B}_{\rm sh}$, where $\boldsymbol{B}_{\rm sh}$ is the magnetic flux density generated by the shielding current density $\boldsymbol{j}_{\rm sh}$. By introducing the magnetic vector potentials $\boldsymbol{A}_{\rm sh}$ and $\boldsymbol{A}_{\rm ex}$, the Maxwell equation (1) becomes equivalent to the following equation:

$$\nabla \times \left(\frac{1}{\mu_0} \nabla \times \boldsymbol{A}_{\rm sh} \right) = -\sigma \frac{\partial}{\partial t} \left(\boldsymbol{A}_{\rm sh} + \boldsymbol{A}_{\rm ex} \right). \tag{6}$$

The edge-based FEM [8] is applied to Eq. (6) to obtain the following equation:

$$K\boldsymbol{a}_{\rm sh} + C(\boldsymbol{a}_{\rm sh}) \frac{d\boldsymbol{a}_{\rm sh}}{dt} = -C(\boldsymbol{a}_{\rm sh}) \frac{d\boldsymbol{a}_{\rm ex}}{dt}, \tag{7}$$

where $\boldsymbol{a}_{\rm sh}$ and $\boldsymbol{a}_{\rm ex}$ are the vectors corresponding to $\boldsymbol{A}_{\rm sh}$ and $\boldsymbol{A}_{\rm ex}$, respectively. Moreover, K and C are the matrixes corresponding to permeability μ_0 and conductivity σ, respectively. Because the conductivity σ in the HTS layer depends on the shielding current density $\boldsymbol{j}_{\rm sh}$, the matrix C also depends on $\boldsymbol{j}_{\rm sh}$. The conductivity σ in the HTS layer is modified in the following iterative procedure until the maximum of $|\boldsymbol{j}_{\rm sh}|$ is converged to $j_{\rm C}$:

$$\begin{cases} \sigma_{\rm new} = \dfrac{j_{\rm C}}{|\boldsymbol{j}_{\rm sh}|}\sigma_{\rm old} & (|\boldsymbol{j}_{\rm sh}| > j_{\rm C}) \\ \sigma_{\rm new} = \sigma_{\rm old} & (|\boldsymbol{j}_{\rm sh}| \leq j_{\rm C}) \end{cases}. \tag{8}$$

Here, $\sigma_{\rm new}$ is the modified conductivity, and $\sigma_{\rm old}$ is the known conductivity. An initial value of $\sigma_{\rm old}$ is assumed to be $\sigma_{\rm old} = j_{\rm C}/E_{\rm C}$, where $E_{\rm C}$ is the critical electric field.

In the present study, Eq. (7) is solved by using the backward difference method and the incomplete Cholesky conjugate gradient (ICCG) method. The shielding current density $\boldsymbol{j}_{\rm sh}$ and the applied magnetic flux density $\boldsymbol{B}_{\rm ex}$ can be determined from the vectors $\boldsymbol{a}_{\rm sh}$ and $\boldsymbol{a}_{\rm ex}$ by the following equations, respectively:

$$\boldsymbol{j}_{\rm sh} = -\sum_{i=1}^{N} \sigma \left(\frac{da_{{\rm sh},i}}{dt} + \frac{da_{{\rm ex},i}}{dt} \right) \boldsymbol{W}_i, \tag{9}$$

$$\boldsymbol{B}_{\rm ex} = \sum_{j=1}^{N} a_{{\rm ex},j} \left(\nabla \times \boldsymbol{W}_j \right). \tag{10}$$

Here, $\boldsymbol{W}_i$ is the shape function of the i-th edge-element ($i = 1, 2, \cdots, N$) and N is the number of the unknowns [9]. Moreover, $a_{{\rm sh},i}$ and $a_{{\rm ex},i}$ are the i-th component of the vectors $\boldsymbol{a}_{\rm sh}$ and $\boldsymbol{a}_{\rm ex}$, respectively. Hence, the Lorentz force $\boldsymbol{F}$ acting on the permanent magnet is obtained by substituting Eqs. (9) and (10) with the following equation:

$$\boldsymbol{F} = \iiint_{V_{\rm sh}} \boldsymbol{j}_{\rm sh} \times \boldsymbol{B}_{\rm ex} \, dV. \tag{11}$$

Here, $V_{\rm sh}$ is the region in which the shielding current density $\boldsymbol{j}_{\rm sh}$ flows.

3. Numerical Results

In this section, the numerical results obtained by the edge-based FEM are shown to investigate the applicability of the permanent magnet method to the multiple HTS tapes. The parameters are fixed as follows: $a = 10$ mm, $b = 10$ μm, $E_{\rm C} = 1$ mV/m, $R_{\rm pm} = 2.5$ mm, $H_{\rm pm} = 3$ mm, $d_{\rm min} = 0.2$ mm, $d_{\rm max} = 20$ mm, and $\tau_0 = 39$ s.

3.1 Relation between maximum repulsive force and critical current density

First, a definition of the maximum repulsive force $F_{\rm M}$ is explained. Figure 5 shows the dependence of the Lorentz force F_z calculated by the FEM code on the distance d. The z-component F_z of the Lorentz force $\boldsymbol{F}$ means an electromagnetic force acting on the permanent magnet. Moreover, the maximum repulsive force $F_{\rm M}$ is defined by the maximum absolute value of F_z. As $F_{\rm M}$ in the case of Fig. 5, $F_{\rm M} = 0.94$ N is obtained.

Next, let us investigate whether the proportional relation of the permanent magnet method is established for

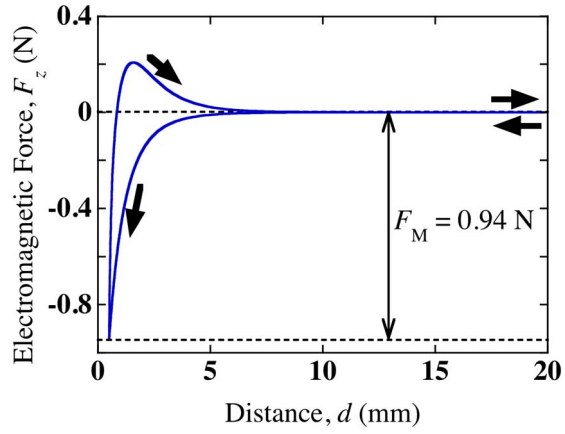

Fig. 5 Dependence of the Lorentz force F_z calculated by the FEM code on the distance d for the case of $L = 1$, $j_C = 10\,\mathrm{kA/mm^2}$, and $B_0 = 0.3\,\mathrm{T}$.

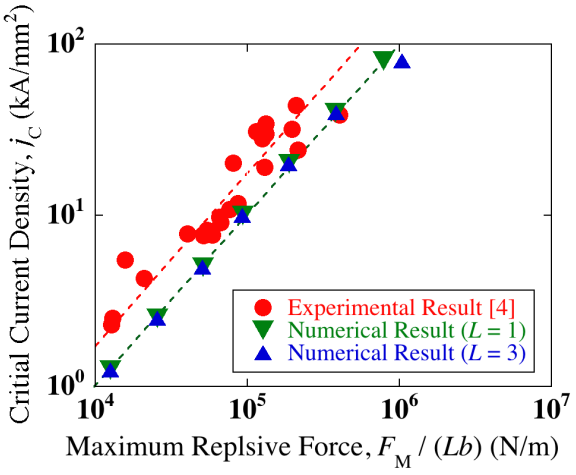

Fig. 6 Dependence of the maximum repulsive force $F_M/(Lb)$ on the critical current density j_C for the case of $B_0 = 0.3\,\mathrm{T}$.

the vertically-stacked multiple HTS tapes. Figure 6 shows the dependence of the maximum repulsive force $F_M/(Lb)$ on the critical current density j_C. The values of $F_M/(Lb)$ obtained by the experiment [4] are also shown in this figure. The experiment was performed for single HTS films of different thicknesses. In order to eliminate the thickness dependency, F_M is divided by the total thickness (Lb) of the HTS layers.

Figure 6 shows that the numerical results for $L = 1$ and $L = 3$ agree qualitatively with the experimental result. However, the numerical results do not agree quantitatively with the experimental result. The study by Takayama *et al.* [5] shows similar results to Fig. 6. Unlike the present study, Takayama *et al.* adopt the n-value model as the superconductive characteristics to simulate the permanent magnet method. However, the numerical results of the present study agree quantitatively with those of Ref. [5]. According to Ref. [5], F_M increases with a decrease in the critical electric field E_C. Therefore, the offset is not due to the J–E constitutive relation (4) and is due to E_C. However, it is extremely difficult to measure E_C in the HTS tape. For this reason, E_C is fixed as $E_C = 1\,\mathrm{mV/m}$, which is commonly used in the simulation [5]. In addition, because the HTS tape in the simulation is an ideal state like single crystal HTS, the numerical result can be regarded as the maximum of F_M that can be taken for each j_C. The finite offset between the numerical and experimental results occurs for the above reasons.

Figure 6 also shows that, as with the experimental result, $F_M/(Lb)$ is proportional to j_C regardless of L. In other words, the permanent magnet method can be applied at least to the case of three HTS tapes.

3.2 Effect of number of HTS tapes on maximum repulsive force

Next, let us investigate an upper limit L_{limit} of the number of the HTS tapes in which the critical current density can be measured. When the shielding current density $|\boldsymbol{j}_{sh}|$ in all the multiple HTS tapes reaches j_C, F_M is proportional to L. On the other hand, when the applied magnetic flux density $\boldsymbol{B}_{ex}$ is sequentially shielded by the HTS tapes close to the permanent magnet, F_M is not proportional to L because $|\boldsymbol{j}_{sh}|$ induced in all the HTS tapes no longer reaches j_C.

Figure 7 shows the dependence of the dimensionless maximum repulsive force F_M/F_{single} on the number of the HTS tapes L. Here, F_{single} denotes a maximum repulsive force for $L = 1$. If the value of F_M/F_{single} is proportional to L, the critical current in the multiple HTS tapes can be measured accurately. Otherwise, the critical current density should not be measured by using the permanent magnet method.

The upper limit L_{limit} is investigated for the case of $B_0 = 0.3\,\mathrm{T}$ (see the red markers in Figs. 7 (a) and 7 (b)). As shown in Fig. 7 (a), for the case of $j_C = 10\,\mathrm{kA/mm^2}$, F_M/F_{single} is not proportional to L for $L > 25$. Namely, the upper limit L_{limit} is $L_{limit} \simeq 25$. As shown in Fig. 7 (b), for the case of $j_C = 20\,\mathrm{kA/mm^2}$, L_{limit} is $L_{limit} \simeq 15$. The upper limit L_{limit} appears to be dependent on j_C. Because a maximum total current which can flow in all the multiple HTS tapes increases with j_C and L, $\boldsymbol{B}_{ex}$ is sequentially shielded by the HTS tapes close to the permanent magnet. Accordingly, L_{limit} decreases with an increase in j_C.

In order to increase L_{limit}, the dependence of F_M/F_{single} on L is investigated for the case with $B_0 = 1\,\mathrm{T}$ (see the blue markers in Figs. 7 (a) and 7 (b)). For the cases of both $j_C = 10\,\mathrm{kA/mm^2}$ and $j_C = 20\,\mathrm{kA/mm^2}$, F_M/F_{single} becomes proportional to L by increasing B_0. For the case of $j_C \leq 20\,\mathrm{kA/mm^2}$, by increasing B_0 to 1 T, the permanent magnet method can be applied at least to the case of 40 pieces of HTS tape. This result is due to an increases in L_{limit}.

3.3 Summary of numerical simulation

Finally, let us summarize the numerical results in

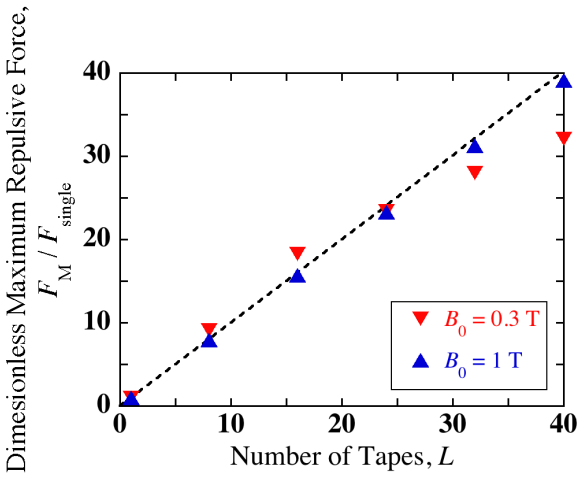

(a) j_C = 10 kA/mm^2

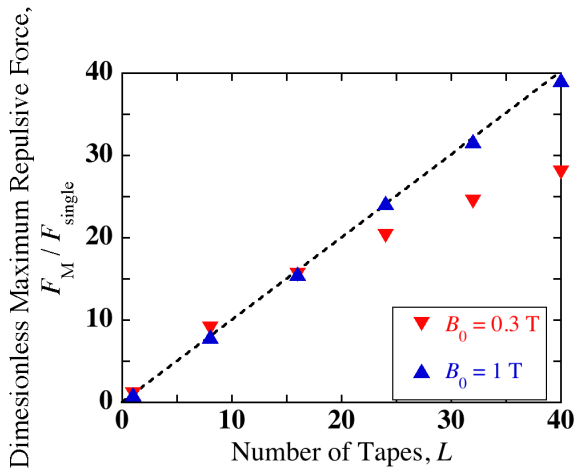

(b) j_C = 20 kA/mm^2

Fig. 7 Dependence of the dimensionless maximum repulsive force F_M/F_{single} on the number of the HTS tapes L.

Figs. 6 and 7. As shown in Fig. 6, $F_M/(Lb)$ is proportional to j_C for the cases with $L = 1$ and $L = 3$. As shown in Fig. 7, for the cases with $B_0 = 0.3$ T, F_M/F_{single} is not always proportional to L. Therefore, the permanent magnet method can be applied to multiple HTS tapes although there is the upper limit L_{limit} of the number of HTS tapes in which j_C can be measured. Moreover, as shown in Fig. 7, F_M/F_{single} becomes proportional to L by increasing B_0 to 1 T. Therefore, by using stronger magnet, the permanent magnet method can measure the critical current density in more stacked HTS tape.

4. Conclusion

We have numerically investigated the applicability of the permanent magnet method to the multiple HTS tapes by using the developed code. Conclusions obtained in the present study are summarized as follows:

- The permanent magnet method can be applied to the multiple HTS tapes although there is an upper limit of the number of HTS tapes in which the critical current density can be measured.
- By using stronger magnet, the permanent magnet method can measured the critical current density when more number of HTS tapes are stacked.

Acknowledgement

This work was performed with the support and under the auspices of the NIFS Collaboration Research program (NIFS21KNSS152).

[1] Y. Shiohara, K. Nakaoka, T. Izumi and T. Kato, J. Japan Inst. Met. Mater. **80**, 406 (2016).
[2] N. Yanagi, S. Ito and Y. Terasaki, J. Cryo. Super. Coc. Jpn. **54**, 10 (2019).
[3] S. Ohshima, K. Takeishi, A. Saito, M. Mukaida, Y. Takano, T. Nakamura, T. Suzuki and M. Yokoo, IEEE Trans. Appl. Supercond. **15**, 2911 (2005).
[4] A. Saito, K. Takeishi, Y. Takano, T. Nakamura, M. Yokoo, M. Mukaida, S. Hirano and S. Ohshima, Physica C **426**, 1122 (2005).
[5] T. Takayama, S. Ikuno and A. Kamitani, IEEE Trans. Appl. Supercond. **18**, 1577 (2008).
[6] M. Tsuchimoto, T. Kojima, H. Waki and T. Honma, Appl. Supercond. **2**, 549 (1994).
[7] M. Tsuchimoto, H. Takeuchi and T. Honma, Trans. IEE Japan **114**, 549 (1994).
[8] R. Albanese and G. Rubinacci, Advances in Imaging and Electron Physics **102**, 1 (1997).
[9] K. Miyata, IEEJ Trans. EIS **124**, 1404 (2004).